Title:	**Performance of Post-Tensioned Slab-Core Wall Connections**
Authors:	Ron Klemencic, Magnusson Klemencic Associates J. Andrew Fry, Magnusson Klemencic Associates Gabriel Hurtado, University of California Berkeley Jack P. Moehle, University of California Berkeley
Subject:	Structural Engineering
Keyword:	Structure
Publication Date:	2006
Original Publication:	PTI Journal 2006 Volume 4 No. 2
Paper Type:	1. **Book chapter/Part chapter** 2. Journal paper 3. Conference proceeding 4. Unpublished conference paper 5. Magazine article 6. Unpublished

PERFORMANCE OF POST-TENSIONED SLAB — CORE WALL CONNECTIONS

RON KLEMENCIC, J. ANDREW FRY, GABRIEL HURTADO, AND JACK P. MOEHLE

ABSTRACT

The use of post-tensioned floor slabs and reinforced concrete core walls has become increasingly popular in high-rise construction. Questions have arisen concerning the performance of this connection when subjected to gravity loads combined with slab-wall rotations consistent with deformation compatibility of building lateral drifts. To address these questions, a test program was conducted at the University of California, Berkeley. Two full-scale specimens indicative of common architectural dimensions and construction details were constructed and subjected to design gravity loads and increasing lateral deformations. The test successfully demonstrated that proposed connection details achieved the Collapse Prevention Performance Objective of 2% interstory drift required by common building codes.

The specimens were subjected to multiple drift cycles of 2.5% and 5% without connection failure. An assessment of the connection's serviceability performance was also made at increasing drift demands. Although significant yielding of the dowel bars was observed in both tests, the yielding did not result in a shear failure of the connection. The connection displayed ductile, flexural performance.

RESEARCH SIGNIFICANCE

The study reported here examines the behavior under earthquake-induced deformations of a widely used connection between slabs and core walls and identifies alternative details that improve the performance of this connection under large rotational demands.

KEYWORDS

core wall; deformation compatibility; Lenton® Form Savers; post-tensioned slab; shear wall, slab–wall connection.

1.0   INTRODUCTION

The use of post-tensioned floor slabs and reinforced concrete core walls has become increasingly popular in high-rise construction in recent years. In many high-rise towers, it is common for the core walls to be constructed ahead of the columns and floor slabs to expedite construction. When this technique is used, a vertical cold-joint is introduced at the slab-wall interface. A common practice is to locate the anchors for the unbonded post-tensioning cables within the slab immediately adjacent to the wall. The slab-wall connection is made through reinforcing dowels placed near the top and bottom of the slab, with mechanical couplers, such as the Lenton® Form Saver, at the slab-wall interface, often supplemented with intermittent shear keys. Figure 1 shows a typical detail.
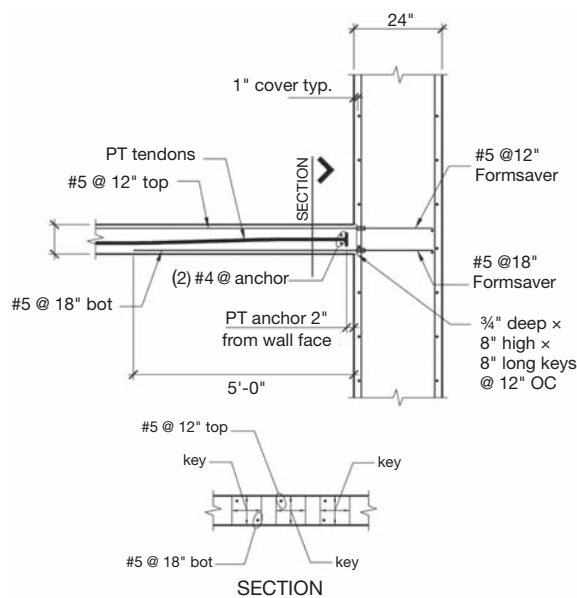

Fig. 1 – Typical Slab-Wall Connection and Detail for Specimen 1

Questions have arisen concerning the performance of this connection when subjected to gravity loads combined with slab-wall rotations consistent with deformation compatibility of building lateral drifts. These questions include:

1. What is the anticipated degree of cracking/damage this connection will display considering various levels of deformation?

2. Does the "lap" between the reinforcing steel dowels and unbonded post-tensioning cables perform adequately?

3. Do the mechanical couplers used for the dowel bars at the interface of the slab and core wall perform adequately considering the prying caused by the rotation of the slab-wall connection?

To address these questions, a test program was conducted at the University of California, Berkeley. Two full-scale specimens indicative of common architectural dimensions and construction details were constructed and subjected to design gravity loads and increasing lateral deformations. Qualitative and quantitative assessments of the performance of the slab-wall connection were made. Based on these test results, adequate performance of the slab-wall connection was confirmed, and detailing improvements are suggested.

2.0 TEST SPECIMENS

Two full-scale specimens were sequentially constructed in the Structures Laboratory at the University of California, Berkeley. The geometry of each specimen was indicative of common architectural dimensions and construction details. Figure 2 illustrates the overall specimen geometry.

The construction sequence of each specimen matched the typical construction sequence followed for many high-rise buildings. First, the full height segment of the core wall and the portion of the column beneath the floor slab were construc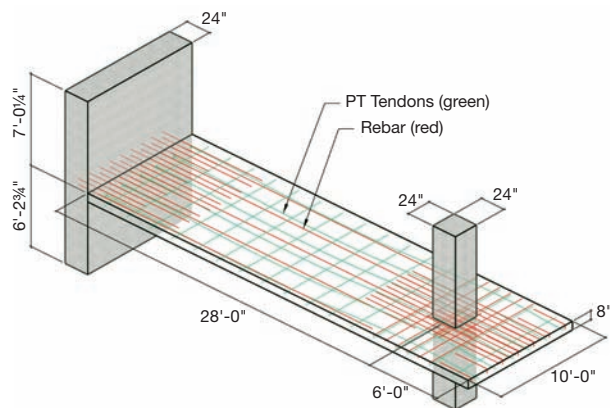ted. Form Savers and intermittent shear keys were installed as part of the wall construction. Installation of formwork, reinforcing steel, and post-tensioning tendons to reinforce the slab followed. Next, concrete was placed and finished for the slab, and the column above the slab was cast. Finally, the post-tensioning tendons were stressed, and formwork and shores removed.

The construction details of both specimens were similar with the exception of the slab-wall connection. As illustrated in Figure 1, the slab-wall connection of Specimen 1 included:

- #5 by 7'-2"-long top dowels at 12" on center
- #5 by 5'-0"-long bottom dowels at 18" on center; the dowels were connected to the wall using Form Saver mechanical couplers
- ¾"-thick by 8"-tall by 8"-long intermittent shear keys at 12" on center
- Post-tensioning tendon anchors placed within 2" of the face of the wall

The slab-wall connection for Specimen 2 was modified in an attempt to enhance the performance of the connection. As illustrated in Figure 3, the slab-wall connection of Specimen 2 included:

- #5 by 7'-2"-long top dowels at 12" on center
- #5 by 3'-2"-long bottom dowels at 12" on center; the dowels were connected to the wall using Form Saver mechanical couplers
- ¾"-thick by 3.5"-tall by 12"-long intermittent shear keys at 24" on center, placed at the mid-depth of the slab
- Post-tensioning tendon anchors placed 8" from the face of the wall

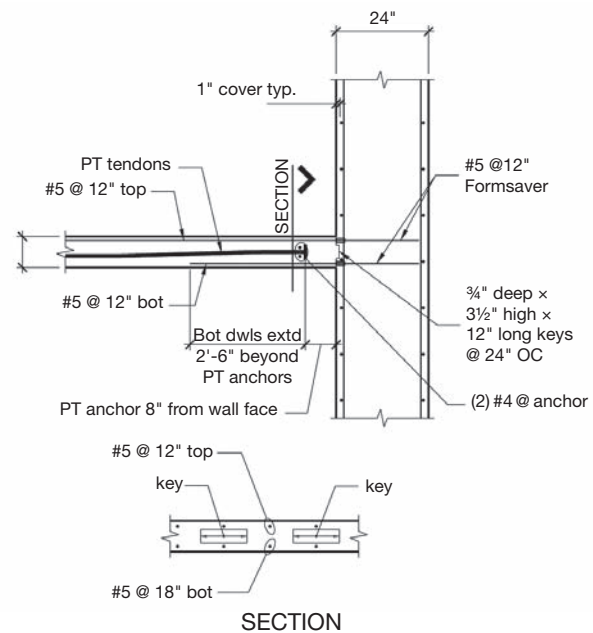Fig. 2 – Isometric Illustration of a Specimen

Fig. 3 – Slab-Wall Connection Detail for Specimen 2

Specimen 1 was constructed to correspond to typical reinforcement details observed in post-tensioned high-rise construction. The larger amount of top bars results from the design boundary condition of fixity between the slab and the wall. For the geometry of the test specimen a small amount of moment redistribution was necessary to substantiate the use of #5 at 12 inches on center top bars.While the performance of Specimen 1 was found to be acceptable, cracking at the slab wall interface occurred at lower drift levels than desired and was concentrated at the slab-wall interface. Specimen 2 was modified in an attempt to delay the onset of cracking, reduce the crack width, and to spread the flexural cracks over a larger distance. The bottom dowels were increased to give the connection equal positive and negative flexural strength. The unequal amount of top and bottom slab dowels in Specimen 1 led to more significant compressive strains in the top reinforcing contributing to what was most likely a fatigue failure of the top dowels at maximum deformation demands.

With equal top and bottom dowel bars, top bar buckling in the zone between the face of the wall at the anchors for the post-tensioning tendons occurred in Specimen 2 at maximum deformation demands. The anchors for the tendons were placed a slab thickness away from the wall to increase the distance over which flexural cracking would occur. Shorter shear keys placed at the mid-depth of the slab were substituted because the slab cracking in Specimen 1 was observed to be more pronounced at each of the full slab-depth shear keys.

Materials for both specimens consisted of A615 Grade 60 reinforcing steel and A416 Grade 270, half-inch diameter unbonded post-tensioning tendons.

For Specimen 1, the average concrete compressive strength of the slab on the day of testing (Day 24) was 7.6 ksi. The concrete mix design is summarized in Table 1.

Table 1 – Concrete Mix Design, Specimen 1 (per cubic yard)

Components/Ingredients	Quantity	Volume (ft³)
RMCPMI Cement–Type II ASTM C150	799 lbs	4.06
Hanson–Angel Island Sand	1431 lbs	8.75
RMCPMI–Clayton ½" ASTM C33	1550 lbs	8.84
Water	292 lbs	4.68
Total Air	2.5 %	0.68
Grace–Recover Retarder	3 oz	0.00
Grace–Adva 100 HR Water Reducer	80 oz	0.00
Total		**27.00**
Properties of the Mix Water/Cementitious Materials Ratio of 0.37 Slump of 7 to 9 in. Concrete Unit Weight of 151 pcf		

For Specimen 2, the average concrete compressive strength of the slab on the day of testing (Day 17) was 6.1 ksi. The concrete mix design is summarized in Table 2.

Table 2 – Concrete Mix Design, Specimen 2 (per cubic yard)

Components/Ingredients	Quantity	Volume (ft³)
Hanson Cement–Type II ASTM C150	494 lbs	2.51
ISG Fly ash–Class "F" ASTM C618	165 lbs	1.15
Hanson–Angel Island Sand	1341 lbs	8.20
Hanson–Sechelt ½" × #4 ASTM C33	1800 lbs	10.72
Water	250 lbs	4.01
Total Air	1.5 ± 0.5%	0.41
Master Builders–Glenium 3030	65.80 oz	0.00
Master Builders–200N ASTM C494	19.74 oz	0.00
Total		**27.00**
Properties of the Mix Water/Cementitious Materials Ratio of 0.38 Slump of 6 in. Concrete Unit Weight of 150 pcf		

3.0 TEST SET-UP

The test setup positioned each specimen atop "pinned" clevises anchored to the laboratory strong floor, with lateral deformations imposed by actuators attached near upper ends of the wall and column (Figure 4). Specimen story height was 10' 8¾", measured from the center of the clevis pin to the centerline of the actuator. To securely connect the specimen to the pinned clevises at the base, additional headed anchor bars were installed at the base plate of the wall (Figure 5) and column (Figure 6). As shown in Figure 5, additional ties were also provided at the base of the wall to confine the headed anchor bars and U-hoops were placed at the edges of the wall along the entire height.
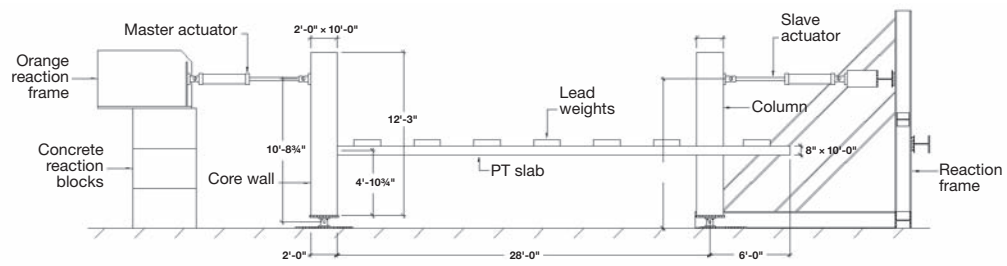
Fig. 4a – Elevation of Test Set-Up
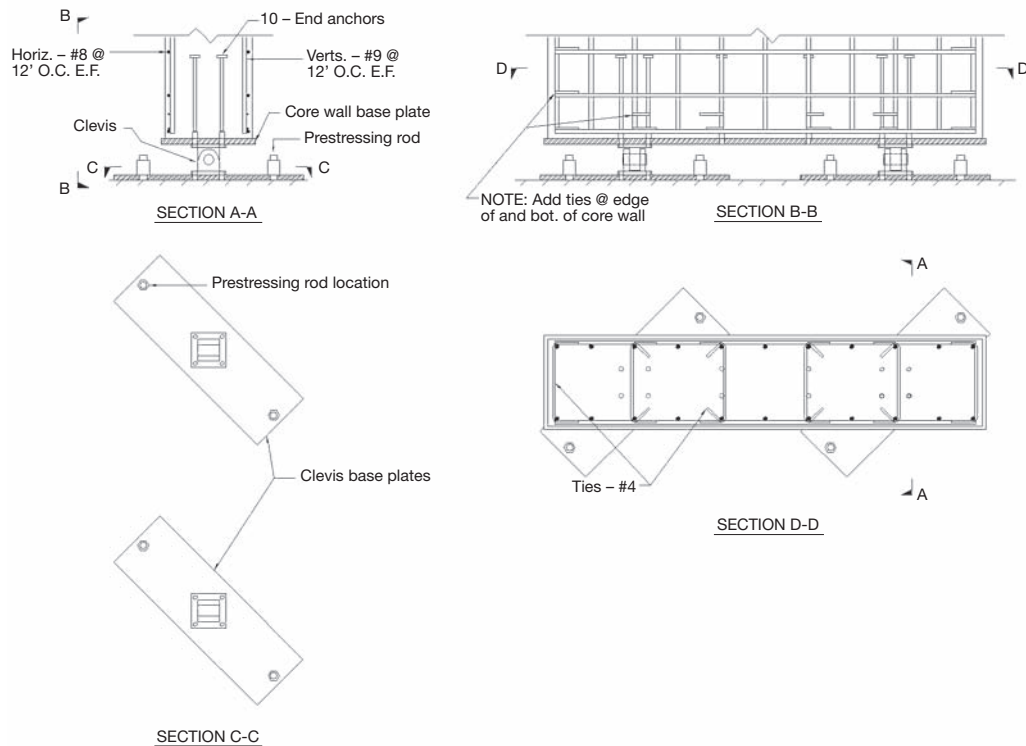

Fig. 4b – Test Set-Up
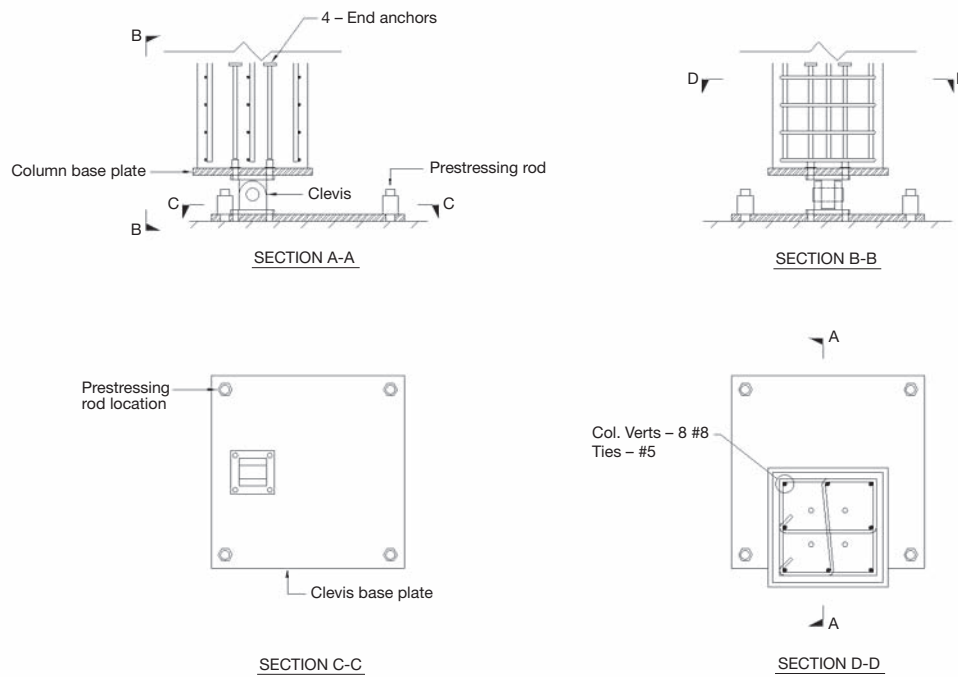

Fig. 5 – Wall-Clevis Connection Detail

SECTION A-A

SECTION B-B

SECTION C-C

SECTION D-D

Fig. 6 – Column-Clevis Connection Detail

Fig. 7 – Instrumentation of Specimens

Table 3 – Instrumentation

Gauge Type	Description
Transducer	Master Actuator Force
Transducer	Slave Actuator Force
Temposonic	Master Actuator Stroke
String-Pot	Slave Actuator Stroke
Cable Cell	Longitudinal Strand (2 through Column)
Cable Cell	Transverse Strand (through Column)
String-Pot	Wall Longitudinal Displacement
String-Pot	Column Longitudinal Displacement
String-Pot	Column Transverse Displacement
String-Pot	Slab Vertical Displacement (¼, ½, and ¾ Span)
Stick-Pot	Top and Bottom of Slab at Slab-Wall Joint
Stick-Pot	Wall at Slab-Wall Joint (¼ and ¾ Wall Length)
Strain Gauge	Dowel #1 (2", 30", and 58" from Wall)
Strain Gauge	Dowel #2 (2", 30", and 58" from Wall)
Strain Gauge	Dowel #3 (2" and 30" from Wall)
Strain Gauge	Dowel #4 (2" and 30" from Wall)

Table 3 summarizes the instrumentation used to gather test data. Figure 7 illustrates the locations of the instrumentation listed in Table 3. Strain gauges on slab bottom bars near midspan and on stud rails near the column were not used in Specimen 2.

4.0 TEST PROTOCOL

Prior to applying lateral deformations to each specimen, 21 bundles of lead weights, each weighing 500 lb, were positioned on the slab, as shown in Figure 8. This corresponds approximately to a superimposed load of 30.5 psf, which is representative of expected loading in high-rise residential construction.

Target lateral displacements were selected to relate to limit states investigated during the design of high-rise buildings. Common engineering practice is to limit the maximum design interstory drift ratio caused by wind loading to H/400 (0.0025H), where H is the story height. For seismic loading, FEMA 356 provides typical drift values associated with Structural Performance Levels. These drift values are 0.5 percent (0.005H) for the Immediate Occupancy Performance Level, 1.0 percent (0.01H) for Life Safety Performance Level, and 2 percent (0.02H) for Collapse Prevention Performance Level. Lateral deformations were increased to a total of 5 percent, well beyond design limitations envisioned by current building code provisions, to test the robustness of the connection. The qualitative performance of each specimen was noted at these various deformation levels.

In tall buildings, axial deformation of the core walls caused by the flexural behavior of the wall assembly increases rotational demands on the slab-wall connection. Considering a building approximately 400-feet tall and a slab span of approximately 30 feet, the effect of this building action causes rotations inducing tension on the top of the slab to be approximately double the rotations inducing tension on the bottom of the slab. This principle is illustrated in Figure 9.

Effects of earthquake deformations were simulated by subjecting the specimens to target lateral displacements at the elevation of the actuators. Positive displacements were consistent with target building drift ratios while negative displacements were increased to account for the axial (tension) deformation of the core wall. The positive displacement direction is defined as displacement in the direction from the wall toward the column (from left to right in Figure 4); positive force is defined in the same direction.
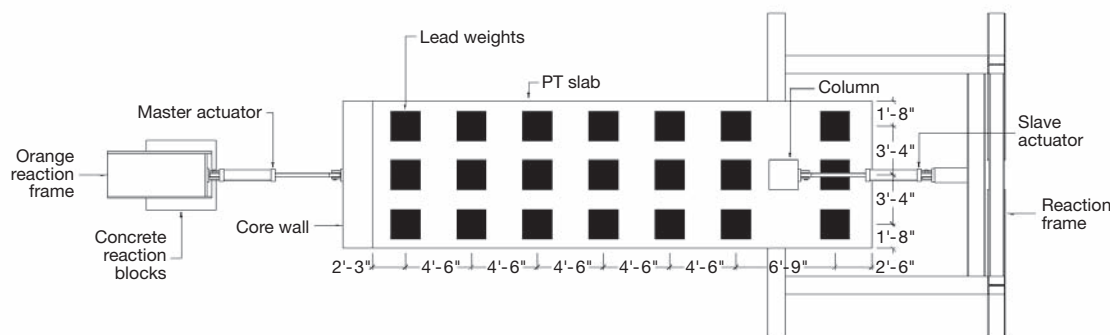

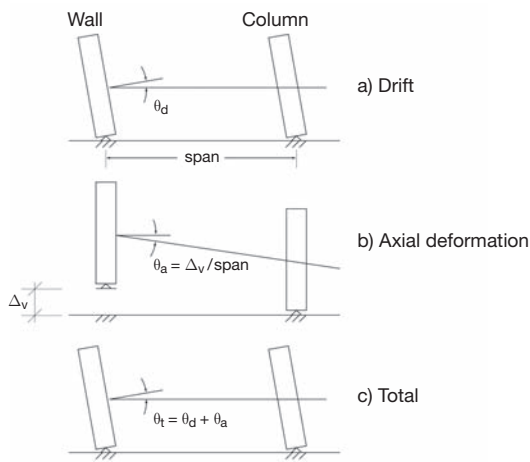Fig. 8 – Plan of Test Set-Up Showing Superimposed Loads

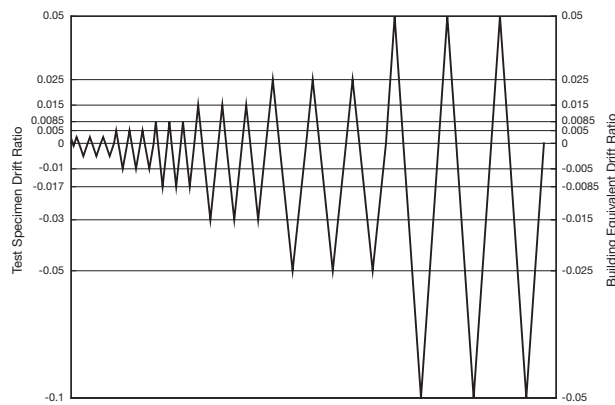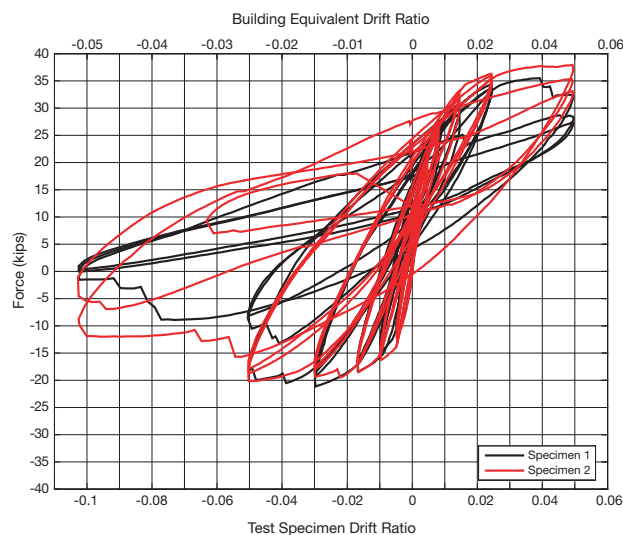Fig. 9 – Supplemental Joint Rotation Due to Vertical Core Wall Deformation

To induce the target lateral displacement protocol, a "master" actuator connected to the core wall was commanded under displacement control with the drift ratio time history shown in Figure 10. The specimen was laterally loaded with a low-level symmetric cycle, followed by six asymmetric cycle groups of increasing drift ratio 0.0025, 0.005, 0.0085, 0.015, 0.025, and 0.05.

A "slave" actuator connected to the column was controlled under force control. The purpose of this actuator was to limit any slab in-plane forces that might otherwise develop due to the boundary conditions of the test set-up. To account approximately for anticipated differences in flexibility of the slab-column connection and the slab-wall connection, the force input to the slave actuator was 70 percent of the force in the master actuator.

Fig. 10 – Drift Ratio History

5.0   RESULTS

Figure 11 shows the total lateral force versus specimen drift ratio for both specimens. Specimen drift ratio is the displacement of the wall divided by the wall height, measured from the center of the pin to the centerline of the actuator. Test specimen drift ratio is equal to building equivalent ratio for positive drifts (drift toward the column side) and twice that value for negative drifts. The scaling factor 2.0 for negative drifts is to account approximately for wall axial (tension) deformation, as discussed in relation to Figure 9. The total lateral force is the sum of the force in the master actuator and slave actuator.

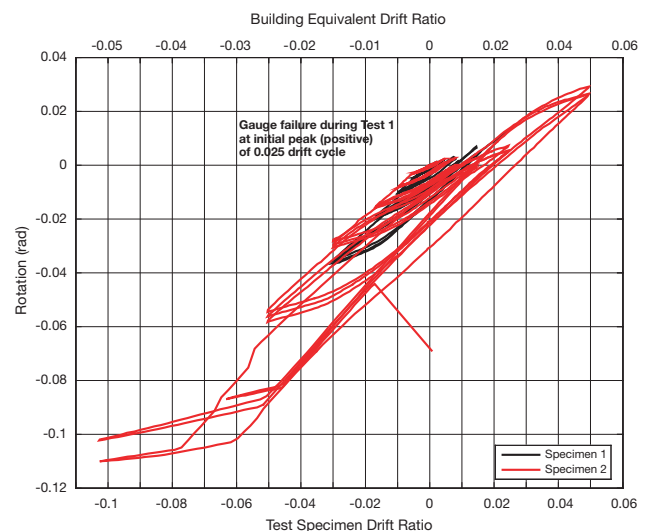Fig. 11 – Total Lateral Force vs. Specimen Drift Ratio for Specimens 1 and 2

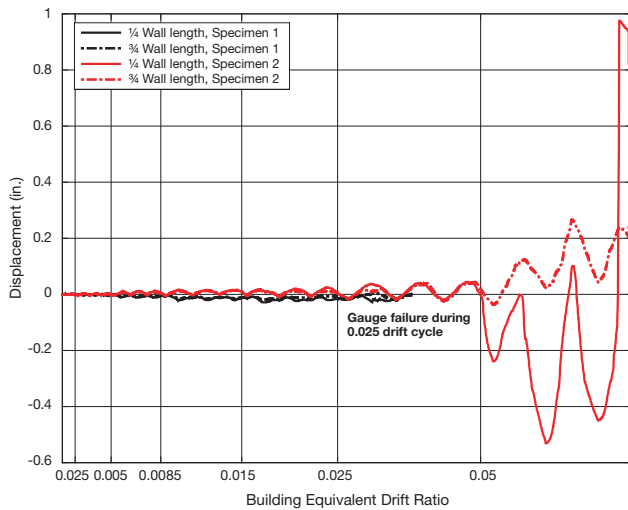Fig. 12 – Slab-Wall Joint Rotation vs. Specimen Drift Ratio for Specimens 1 and 2

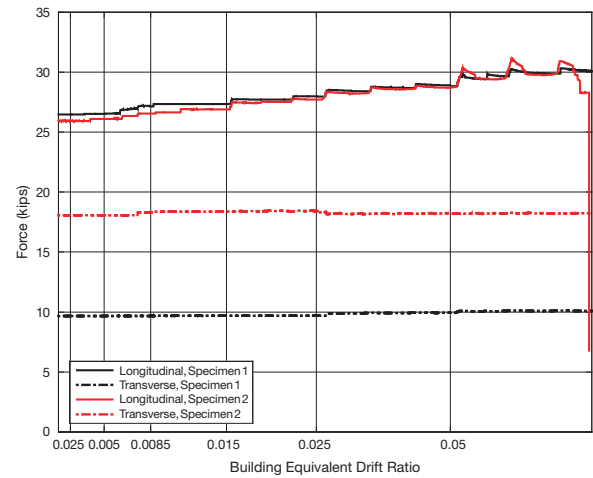Fig. 13 – Slab-Wall Joint Vertical Displacement for Specimens 1 and 2

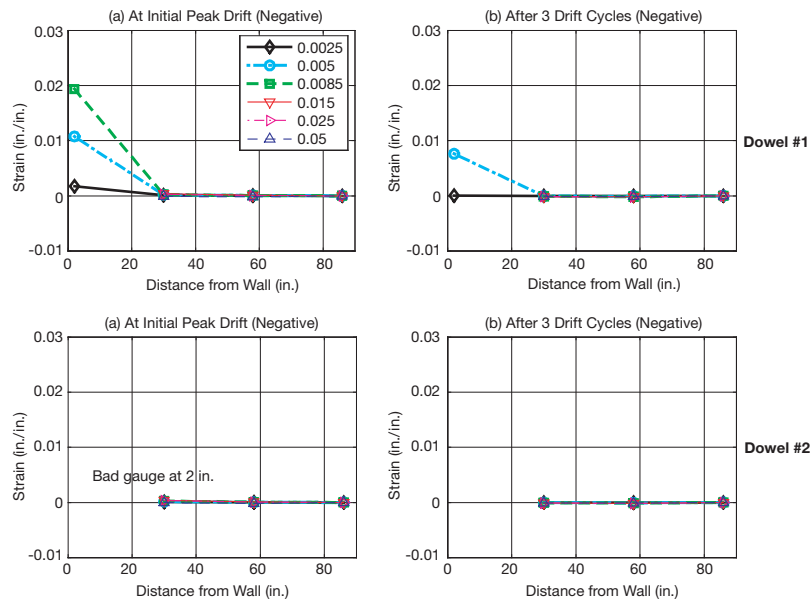Fig. 14 – Post-Tensioned Strand Force for Specimens 1 and 2

Fig. 15 – Specimen 1: Top Dowel Strain Profile

Figure 12 shows the slab-wall joint rotation versus specimen drift ratio for both specimens. To measure rotations, stick-pots were fixed to the top and bottom slab surfaces with targets to the wall face. Slab-wall rotation is defined as the difference in displacement readings from the stick-pots divided by the vertical distance between them. Referring to Figure 12, the stick-pot connection at the top of the slab failed in Specimen 1 due to spalling of the concrete slab during the initial peak positive displacement of the 0.025 specimen drift ratio cycle, limiting the test data necessary to compute the slab-wall joint rotation at larger drift ratios.

The stick-pot on the top of the slab in Specimen 2 moved off its target during the 0.05 specimen drift ratio cycle due to spalling of the concrete slab. Thus, measured rotations beyond the 0.05 drift cycle should be considered as approximations.

Figure 13 shows the variation of vertical movement at the slab-wall joint as a function of building equivalent drift ratio for both specimens. Vertical movement is defined as the vertical displacement of the slab relative to the wall, as measured by stick-pots fixed to the wall face and targeting the underside of the slab. The horizontal axis of the figure corresponds to the initial peak positive specimen drift ratio. Spalling of the concrete slab made the measurements inaccurate toward the end of the test for Specimen 1; therefore, data are shown only through the 0.025 drift cycle.
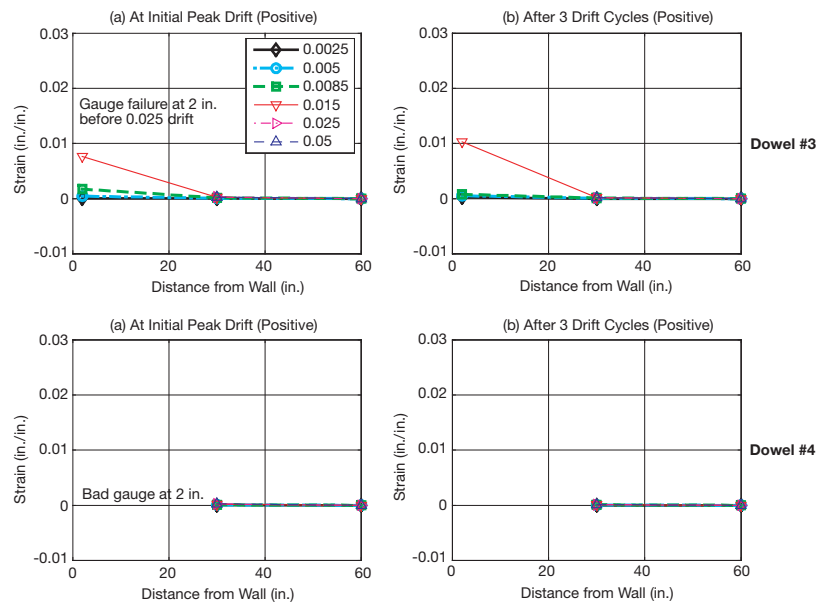
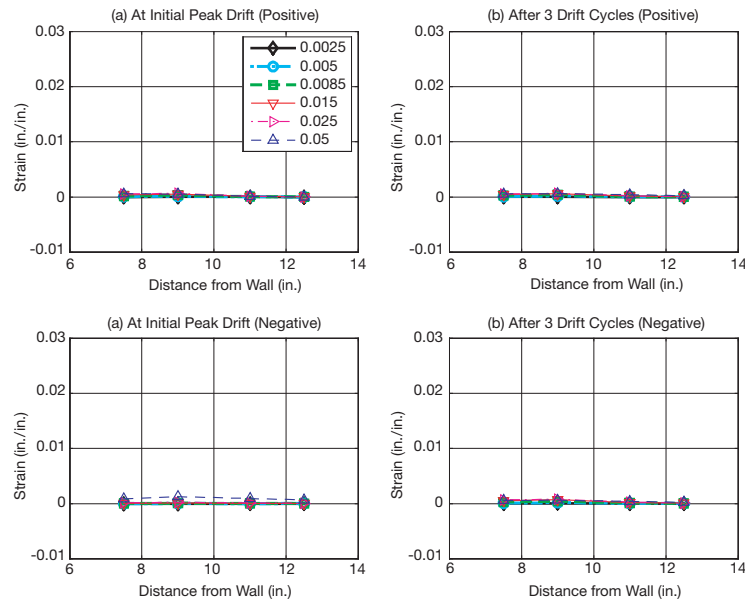**Fig. 16 – Specimen 1: Bottom Dowel Strain Profile**

Fig. 17 – Specimen 1: Bottom Bar Strain Profile

For Specimen 2, the variation in movement at the quarter and three-quarter wall locations during the 0.05 building equivalent drift ratio cycle was due to spalling of the slab at the location of the gauges.

Figure 14 shows the post-tensioned cable force as a function of building equivalent drift ratio for both specimens. The strand force in the longitudinal and transverse directions did not vary significantly at increasing drift ratios. The large dropoff in force in the PT tendon in Specimen 2 was the result of a large crack that developed in the specimen roughly 8 feet from the column during the third cycle of 0.05 building equivalent drift.

5.1 SPECIMEN 1 REINFORCING STEEL STRAIN PROFILES

Figures 15, 16, and 17 show the strain profiles along the top dowels (dowels #1 and #2), bottom dowels (dowels #3 and #4), and bottom bars at key equivalent building drift ratios (indicated in the legend), respectively. The largest strains in the top and bottom dowels occurred near the wall face; the strains were effectively zero at gauge locations 30 inches from the wall face and beyond. Referring to Figure 17, the bottom bars underwent very small strains along the bar length that was instrumented.
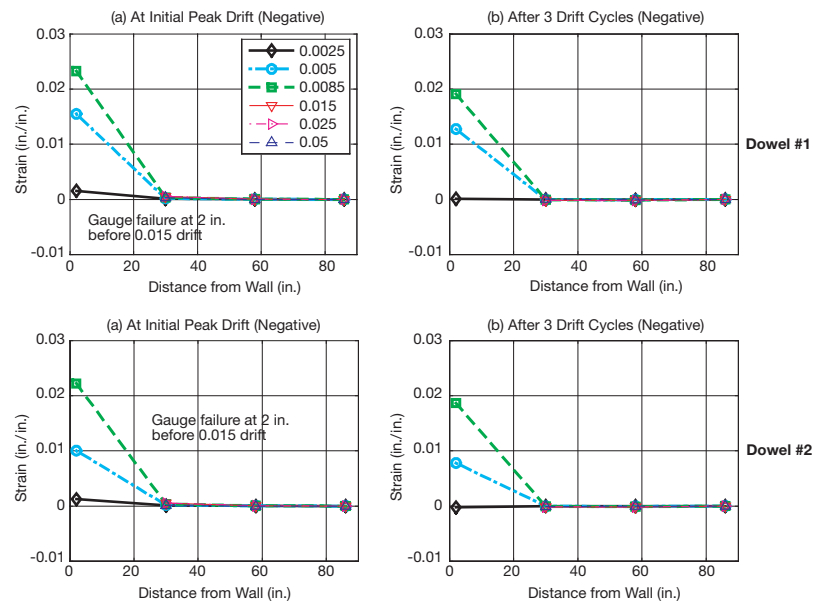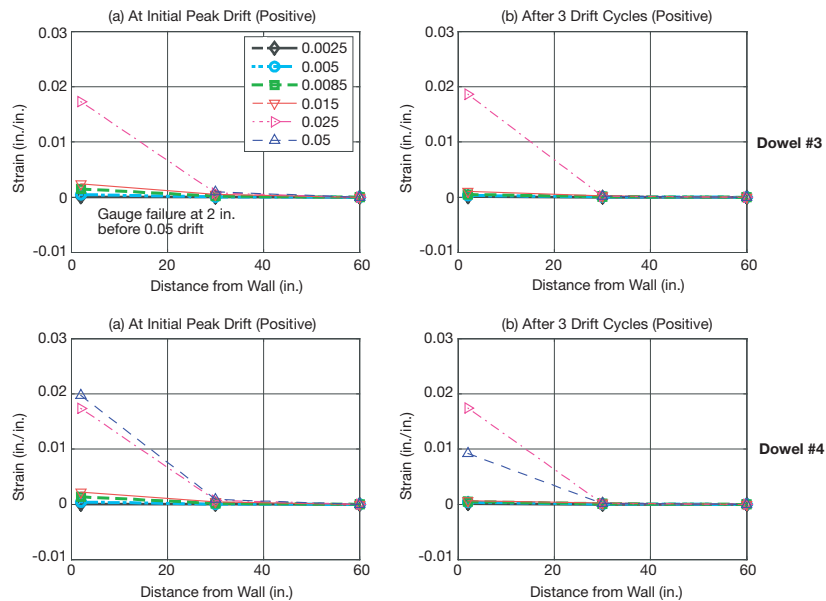
Fig. 18 – Specimen 2: Top Dowel Strain Profile

Fig. 19 – Specimen 2: Bottom Dowel Strain Profile

5.2 SPECIMEN 2 REINFORCING STEEL STRAIN PROFILES

Figures 18 and 19 show the strain profiles along the top dowels (#1 and #2) and bottom dowels (#3 and #4), respectively. The highest strains in the top and bottom dowels occurred near the face of the wall, with effectively zero strain recorded at other gauge locations.

Figure 20 shows the variation of strain on the studs near the column (see Figure 7 for location of instrumentation) as a function of building equivalent drift ratio for Specimen 1. The horizontal axis of Figure 20 corresponds to the initial peak positive drift ratio in each drift cycle. Clearly, the studs experienced very small strains during the test.

5.3 COMPARISON OF PEAK LATERAL FORCES

Table 4 summarizes the total lateral force required at the first and third peaks in the positive and negative directions for Specimens 1 and 2. As seen in Figure 11, and highlighted in Table 4, the most dramatic difference in the two tests occurred during the 0.025 and 0.05 building equivalent drift ratio cycles. The total lateral force required to reach the third peak in the negative direction of the 0.025 drift cycle was -7.8 kips and -16.6 kips for Specimens 1 and 2, respectively. The total lateral force required to reach the first peak in the negative direction of the 0.05 drift cycle was -0.9 kips and -8.8 kips for Specimens 1 and 2, respectively.
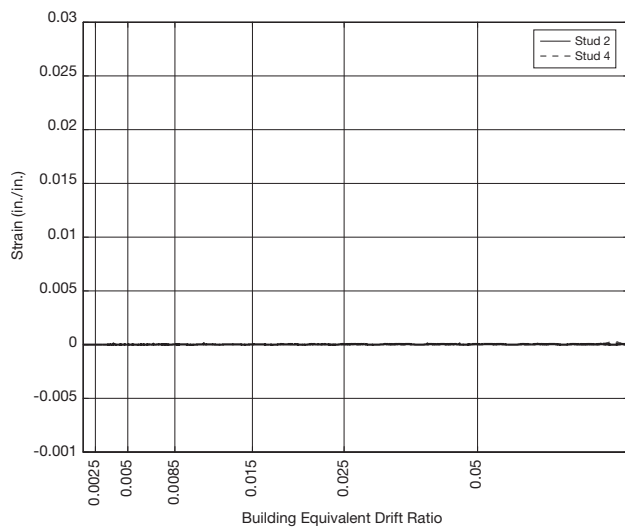
Fig. 20 – Stud Rail Strain for Specimen 1

Table 4 – Total Lateral Force at Peak Equivalent Building Drift Ratios

Building Equivalent Drift Ratio	Direction	Peak	Specimen 1 Total Lateral Force (kips)	Specimen 2 Total Lateral Force (kips)
0.0025	Positive	1st	12.2	12.3
		3rd	15.8	10.6
	Negative	1st	-8.3	-10.6
		3rd	-9.5	-11.9
0.005	Positive	1st	19.9	16.1
		3rd	22.6	19.1
	Negative	1st	-12.7	-14.4
		3rd	-12.6	-13.9
0.0085	Positive	1st	20.6	23.3
		3rd	24.8	25.0
	Negative	1st	-16.5	-16.2
		3rd	-16.0	-15.9
0.015	Positive	1st	26.0	29.7
		3rd	30.1	31.7
	Negative	1st	-19.9	-17.4
		3rd	-17.9	-16.2
0.025	Positive	1st	33.4	34.4
		3rd	33.1	34.2
	Negative	1st	-17.4	-18.2
		3rd	-7.8	-16.6
0.05	Positive	1st	31.9	36.9
		3rd	27.0	32.5
	Negative	1st	-0.9	-8.8
		3rd	1.0	Not completed

Table 5 – Maximum Crack Width (inches) of Slab Near Wall

Building Equivalent Drift Ratio	Location	Maximum Crack Width (inches) with Specimen Held at Peak Drift	
		Specimen 1	Specimen 2
0.0025	Top of Slab	0.016	0.020
	Bottom of Slab	0	0
0.005	Top	0.040	0.060
	Bottom	0.010	0
0.0085	Top	0.080	0.130
	Bottom	0.013	0.013
0.015	Top	0.200	0.190
	Bottom	0.030	0.013
0.025	Top	1.000	0.560
	Bottom	0.200	0.020
0.05	Top	-	-
	Bottom	-	-

The maximum crack widths measured at the top and the bottom of the slab near the wall at the completion of each drift cycle for Specimens 1 and 2 are summarized in Table 5. Figures 21 and 22 show the crack patterns for Specimins 1 and 2 respectively at various drift levels. Crack widths were not measured for the 0.05 equivalent building drift ratio cycle. The crack widths reported in Table 5 are indicative of the maximum measured cracks near the face of the wall as the imposed lateral deformation level was held at its peak value. When Specimen 2 was re-centered after the third 1.5 percent building equivalent drift cycle, these cracks closed and did not display evidence that repair would be required. In Specimen 2, the cracks remained "repairable" after the third 2.5 percent building equivalent drift cycle. The cracks also closed in Specimen 1 when it was re-centered, but the damage observed at the slab-wall interface after the third 1.5 percent building equivalent drift cycle would likely have required repair.

The type of failure, if any, of the dowel bars for Specimens 1 and 2 is summarized in Table 6 and Table 7, respectively. For Specimen 2, three top dowel bars fractured, corresponding to three popping sounds during the test, one pop en route to the first negative peak of the 0.015 drift cycle and two pops en route to the first negative peak of the 0.05 drift cycle. The dowel bar fractures can also be observed in Figure 11 where the total force drops sharply near (-0.023 specimen drift ratio, -18 kips), (-0.056 specimen drift ratio, -12 kips), and (-0.067 specimen drift ratio, -11 kips). The dowel bar marks are shown in Figures 21 and 22 for Specimens 1 and 2 respectively.

a) Cracking at Top of Slab at 0.5% Drift (Specimen Held at Peak Rotation)

c) Cracking at Top of Slab at 2.5% Drift (Specimen Held at Peak Rotation)

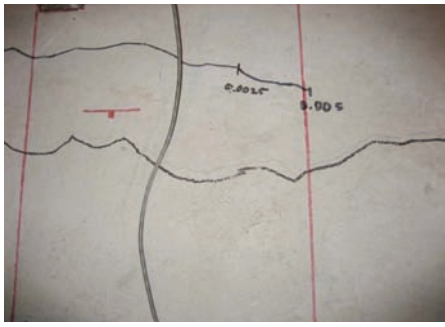b) Cracking at Top of Slab at 1.5% Drift (Specimen Held at Peak Rotation)

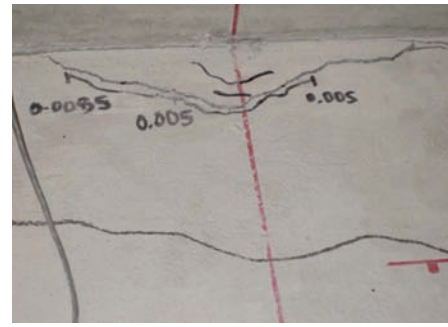d) Cracking at Top of Slab at 5.0% Drift (Specimen Held at Peak Rotation)

e) Zero Displacement After 5.0% Drift (Specimen Held at Peak Rotation)
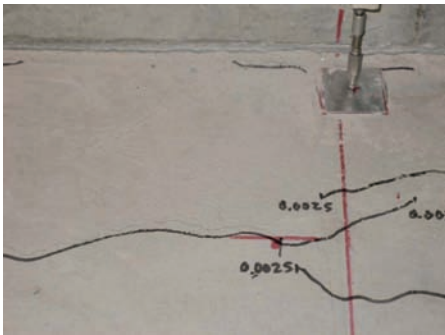
Fig. 21 – Cracking Patterns for Specimen 1 at Various Drift Levels

a) Cracking at Top of Slab at 0.5% Drift
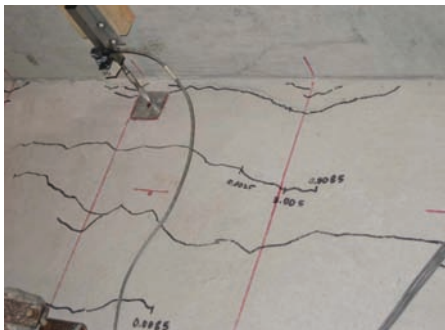   (Specimen Held at Peak Rotation)

e) Cracking at Top of Slab at 1.5% Drift
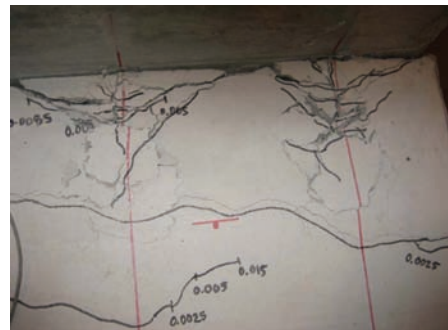   (After 3 Cycles and Return to Initial Position)

b) Cracking at Top of Slab at 0.85% Drift
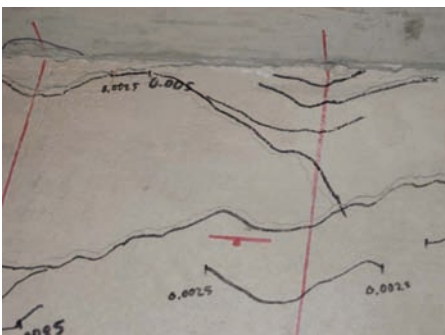   (Specimen Held at Peak Rotation)

f) Cracking at Top of Slab at 2.5% Drift
   (Specimen Held at Peak Rotation)

c) Cracking at Top of Slab at 0.85% Drift
   (After 3 Cycles and Return to Initial Position)

g) Cracking at Top of Slab at 2.5% Drift
   (After 3 Cycles and Return to Initial Position)

d) Cracking at Top of Slab at 1.5% Drift
   (Specimen Held at Peak Rotation)

h) Cracking at Top of Slab at 5.0% Drift
   (Specimen Held at Peak Rotation)

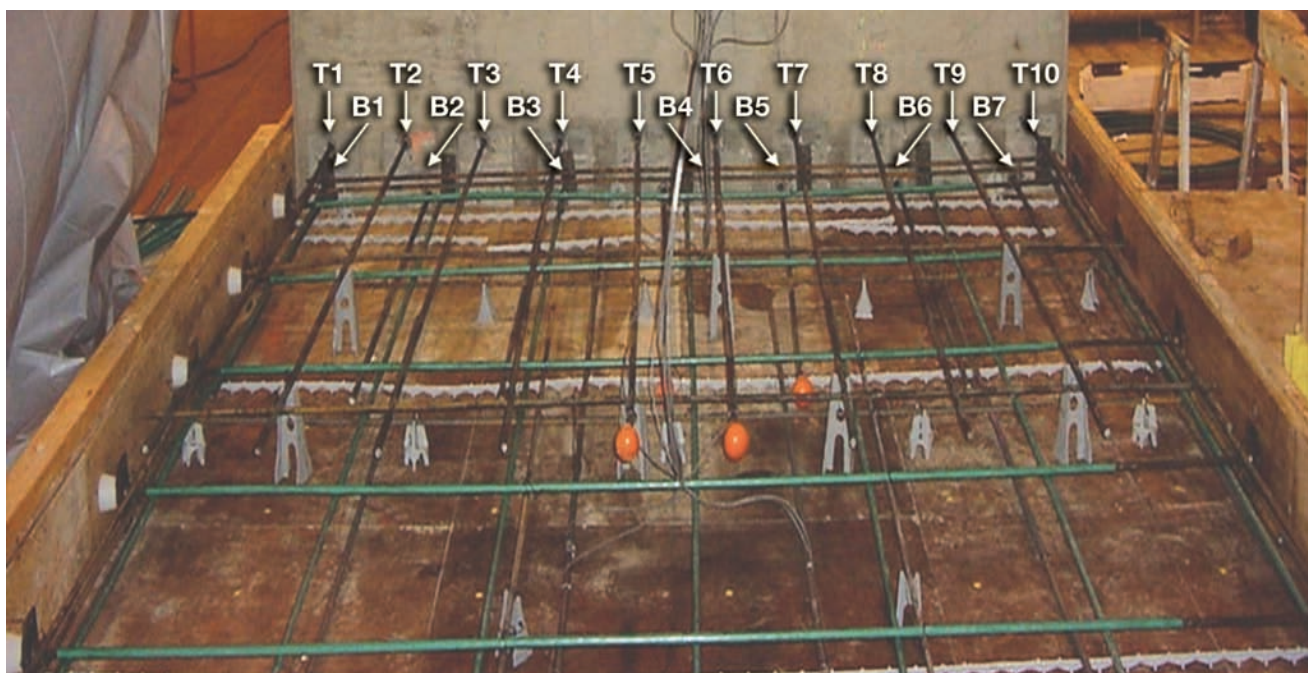Fig. 22 – Cracking Patterns for Specimen 2 at Various Drift Levels
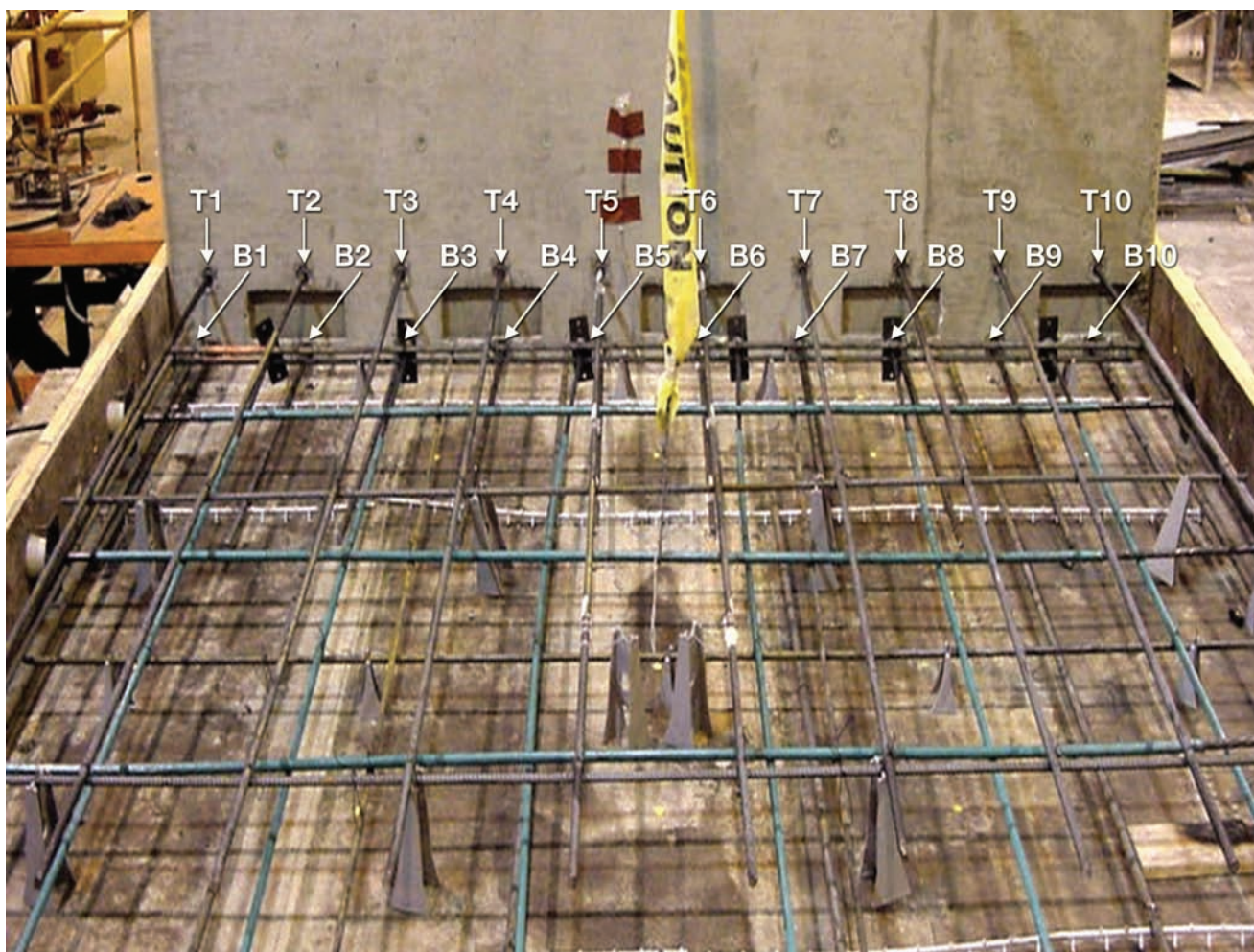
Fig. 23 – Dowel Bar Legend: Specimen 1

Fig. 24 – Dowel Bar Legend: Specimen 2

Table 6 – Type of Dowel Bar Failure: Specimen 1

Dowel	Type of Failure
T1	Pull-out of dowel @ thread
T2	Pull-out of form saver
T3	Pull-out of form saver
T4	Pull-out of dowel @ thread
T5	Pull-out of dowel @ thread
T6	Fracture of dowel @ 3" from wall
T7	Pull-out of form saver
T8	Pull-out of dowel @ thread
T9	Fracture of dowel @ thread
T10	Pull-out of dowel @ thread
B1	Yielding of dowel
B2	Yielding of dowel
B3	Yielding of dowel
B4	Yielding of dowel
B5	Yielding of dowel
B6	Yielding of dowel
B7	Yielding of dowel

Table 7 – Type of Dowel Bar Failure: Specimen 2

Dowel	Type of Failure
T1	Buckling and fracture of dowel @ thread
T2	Buckling of dowel
T3	Buckling of dowel
T4	Buckling of dowel
T5	Buckling of dowel
T6	Yielding of dowel
T7	Yielding of dowel
T8	Fracture of dowel @ thread
T9	Yielding of dowel
T10	Buckling and fracture of dowel @ thread
B1	Yielding of dowel
B2	Yielding of dowel
B3	Yielding of dowel
B4	Yielding of dowel
B5	Yielding of dowel
B6	Yielding of dowel
B7	Yielding of dowel
B8	Yielding of dowel
B9	Yielding of dowel
B10	Yielding of dowel

6.0   DISCUSSION

6.1   OVERALL PERFORMANCE

One of the primary objectives of these tests was to demonstrate the proposed connection details achieved a Collapse Prevention Performance Objective at deformation levels consistent with drift limits specified in common building codes, typically a 2 percent interstory drift. Both specimens were subjected to multiple drift cycles of 2.5 percent and 5 percent drift without failure of the slab wall connection. See Figure 25.
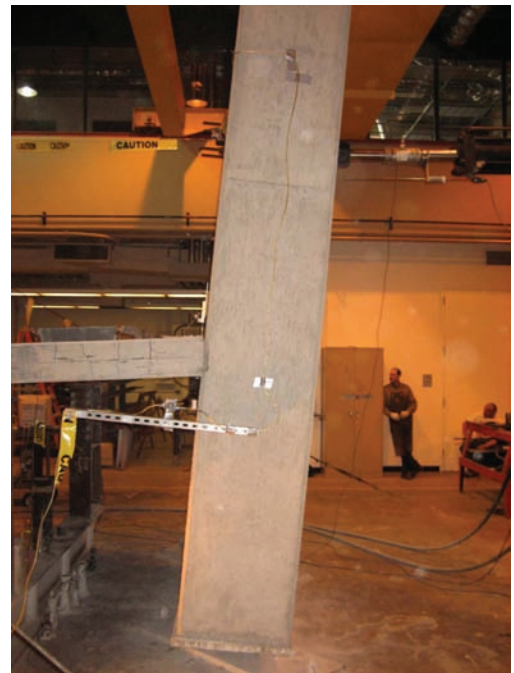

Fig. 25 – Minimum Rotation Demand in Specimens 1 & 2

As seen in Figure 11, the connection remained essentially elastic in both specimens through three cycles of the 0.85 percent building equivalent drift ratio. Inelastic behavior was observed to occur in both specimens at approximately 1.0 percent building equivalent drift ratio. Thus it can be inferred that for building drifts experienced in conjunction with an overall Life Safety Performance Level, the connection will remain elastic or nearly elastic.

Significant flexural strength loss in the connection was observed to occur in Specimen 1 after the first cycle of 2.5 percent building equivalent drift. This resulted from a number of pull-out failures of the top dowels as listed in Table 6. Significant flexural strength loss was observed in Specimen 2 during the first cycle of 5 percent building equivalent drift (strength loss occurred at approximately 2.75 percent building equivalent drift). Only three of the ten top dowels fractured in Specimen 2, as listed in Table 7. Therefore, Specimen 2 retained considerably more flexural strength in the slab-wall connection than Specimen 1.

Significant flexural strength loss was not observed in either specimen during positive motions (tension in the bottom of the slab at the slab-wall connection). While yielding of the bottom dowels was observed at building equivalent drift of 1.5 to 2 percent, none of the bottom dowels fractured or experienced a pull-out failure in either test. Even after three cycles of building equivalent drift of 5 percent, well in excess of code expectations, the bottom dowels provided a positive means of transferring the shear loads from the slab to the wall, consistent with expectations of a Collapse Prevention Performance Level.

Throughout both tests, qualitative and quantitative assessments of crack widths were made at increasing drift demands in order to characterize the serviceability performance of the connection. The crack widths reported in Table 5 are indicative of the maximum measured cracks near the face of the wall as the imposed lateral deformation level was held at its peak value. At low drift ratio levels, hairline cracks appeared first on the top of the slab near the anchors of the post-tensioning tendons. These cracks closed upon re-centering of each specimen.

As building equivalent drift ratios increased to 1.5 percent, additional cracks formed between the face of the core wall and the post-tensioning tendon anchors. When Specimen 2 was re-centered after the third 1.5 percent building equivalent drift cycle, the cracks closed and did not display evidence that repair would be required. In Specimen 2, the cracks remained "repairable" after the third 2.5 percent building equivalent drift cycle. The cracks also closed in Specimen 1 when it was re-centered, but the damage observed at the slab-wall interface after the third 1.5 percent building equivalent drift cycle would likely have required repair.

As building equivalent drift ratios increased beyond 2.5 percent, significant cracking and spalling of the top surface of the concrete slab was observed. The cracks in Specimen 1 were significantly larger and more concentrated than Specimen 2. Buckling and fracture of some of the top reinforcing steel dowels was observed in both tests at drifts exceeding 2.5 percent. Photographs of the cracking of the top of the slab follow at the end of this report.

6.2   COMPARISON OF SPECIMEN 1 AND 2

The most significant difference in performance observed between Specimens 1 and 2 was the degree of cracking on the top slab surface near the face of the wall. In Specimen 1, where the anchors for the post-tensioning tendons were placed only 2 inches from the face of the wall, large cracks were concentrated between the anchor and the wall. In Specimen 2, the anchors for the post-tensioning tendons were placed 8 inches from the face of the wall. The cracks in Specimen 2 were more distributed and narrower.

Another difference in performance was observed related to the performance of the reinforcing steel dowels at larger drift levels. The top reinforcing steel dowels in Specimen 1 failed through bar fracture or pull-out from the Form Savers, while in Specimen 2, the top dowels typically failed due to bar buckling at drift ratios beyond 2.5 percent. The difference in behavior is attributed to the amount of bottom dowel reinforcing in each specimen. The unequal amount of top and bottom slab dowels in Specimen 1 led to more significant compressive strains in the top reinforcing contributing to what was most likely a fatigue failure of the top dowels. With equal top and bottom dowel bars, top bar buckling in the zone between the face of the wall at the anchors for the post-tensioning tendons occurred in Specimen 2.

6.3   BEHAVIOR OF LAP, DOWEL BARS, AND FORM SAVERS

As shown in Figures 15 to 19, the strain levels in the reinforcing steel diminished rapidly only a short distance from the face of the core wall. There was no visual evidence in either test of any cracking or distress related to the "lap" condition between the dowels and the post-tensioning tendons. As shown in Figure 14 the force level in the post-tensioning cables increased by only 10 to 15 percent throughout the duration of both tests.

Although significant yielding of the dowel bars was observed in both tests, this yielding did not result in the complete shear failure of the connection. Rather, the connection displayed ductile, flexural performance.

Pull-out from the Form Savers of some of the top dowel bars in Specimen 1 was observed at building equivalent drift levels in excess of 1.5 percent. This behavior was substantially improved in Specimen 2, where the anchors for the post-tensioning tendons were positioned 8 inches from the face of the wall and an equal amount of top and bottom dowels were included.

6.4   SHEAR STUDS

The low level of demand recorded on the shear studs at the slab-column connection is attributed to the limited width of the specimens. Each specimen's total width of 10 feet represents approximately one-third of a typical slab span, thus the gravity shear stress on the slab-column connection was approximately one-third of a typical condition. As the slab-column connection was not the focus of these tests, the lower level of loading was deemed acceptable and did not affect the results of the slab-wall connection assessment.

7.0   CONCLUSIONS

1. Both specimens for the slab-wall connection met performance expectations at low, moderate, and maximum drift demands.

2. The revised details of Specimen 2 displayed marked improvement in performance as compared to Specimen 1. Revisions in the slab-wall connection detail included:

   a. Placing the anchors for the post-tensioning cables a distance equal to one slab depth away from the face of the wall

   b. Bottom dowels were increased to provide an equal amount of top and bottom reinforcing steel dowels

   c. The shear key detail was revised to include smaller keys centered in the slab depth.

8.0   ACKNOWLEDGEMENTS

Ron Klemencic is President of Magnusson Klemencic Associates in Seattle, Wash. He received a Bachelor of Science in Civil Engineering from Purdue University and a Master of Science in Structural Engineering from the University of California Berkeley. He is past Chairman of both the Council on Tall Buildings and Urban Habitat, and ACI Committee 374: Performance-Based Seismic Design of Reinforced Concrete Buildings, and a member of ACI 318 Sub-Committee H: Seismic Provisions, and ACI 318: Structural Concrete Building Code.

J. Andrew Fry is a Senior Associate with Magnusson Klemencic Associates in Seattle, Wash. He received a Bachelor of Science in Civil Engineering from University of Illinois Urbana-Champaign and a Master of Science in Structural Engineering from the University of California Berkeley. He has designed high-rise core wall buildings in Seattle, San Francisco, and Chicago.

Gabriel Hurtado is a Ph.D. candidate at the University of California Berkeley. He received his Bachelor of Science, Summa Cum Laude, in Civil Engineering from California Polytechnic State University and his Master of Science in Structural Engineering from UC Berkeley. His awards include an American Institute of Steel Construction Structural Steel Educational Council Fellowship, the American Society of Civil Engineers' Arthur S. Tuttle Memorial Scholarship, and a Concrete Reinforcing Steel Institute Fellowship.

Jack P. Moehle is Professor of Structural Engineering and Director of the Pacific Earthquake Engineering Research Center at the University of California, Berkeley. He received his graduate degrees from the University of Illinois at Urbana-Champaign. He is Chair of Subcommittee H, Seismic Provisions, of ACI 318. His professional interests include seismic design and behavior of concrete structures.